RESEARCH ARTICLE

A Comparative Study on Drag Reduction Methods for Continental Shale Drilling in the Fuxing Block, Southeastern Sichuan Basin

Yunfeng Hu[1] **and Ye Yang**[2,*]

[1] Technology Development Department, Sinopec Jianghan Engineering Company, Wuhan 430024, China
[2] Drilling Company No.1 of Sinopec Jianghan Petroleum Engineering Co., Ltd., Qianjiang 433123, China

Abstract

Extended-reach horizontal wells in continental shale formations of the Fuxing Block, southeastern Sichuan Basin, face prominent challenges, including drag and torque exceeding 50 metric tons and difficulties in weight-on-bit (WOB) transfer. Continental shale is characterized by high porosity, high permeability, distinct amphiphilic properties, and rapid performance degradation of oil-based drilling fluids (OBDF). These features lead to the formation of thick filter cakes and compacted cuttings beds, which further exacerbate abnormal drag. Existing research often focuses on single technical aspects, lacking integrated, full-cycle multi-factor coupling analysis. Based on field data from 14 drilled wells in the block, this study standardizes key factors through data preprocessing, quantifies process weights using the Analytic Hierarchy Process (AHP) model, and fits censored drag data via the Reliability Analysis model. Results indicate that design optimization contributes most significantly to drag reduction (weight: 0.5499). The critical failure drag for encapsulated lubricants is identified as 61.74 t. For wells with horizontal sections exceeding 2500 m, the application of floating casing technology enhances drag control reliability.

Keywords: continental shale, horizontal well, drag/torque, AHP model, reliability analysis model.

1 Introduction

Drilling horizontal wells in shale oil and gas reservoirs involves multiple technical challenges [1]. Complex variations in wellbore curvature demand strict trajectory control precision, while poor formation drillability results in low rates of penetration (ROP). Furthermore, the interaction between swelling minerals (e.g., montmorillonite) in shale and conventional water-based muds can accelerate formation swelling, increasing the risk of wellbore instability. These issues collectively lead to abnormally high drag and torque, severely restricting drilling efficiency and safety [2–4]. Thus, quantitative evaluation of block-specific drag reduction techniques holds great practical significance.

Regarding macroscopic analytical approaches, Wang

Submitted: 28 December 2025
Accepted: 07 February 2026
Published: 28 February 2026

Vol. 2, **No.** 2, 2026.
10.62762/RS.2025.790790

***Corresponding author:**
✉ Ye Yang
kalimoto1977@yeah.net

Citation
Hu, Y., & Yang, Y. (2026). A Comparative Study on Drag Reduction Methods for Continental Shale Drilling in the Fuxing Block, Southeastern Sichuan Basin. *Reservoir Science*, 2(2), 81–96.

© 2026 by the Authors. Published by Institute of Central Computation and Knowledge. This is an open access article under the CC BY license (https://creativecommons.org/licenses/by/4.0/).

et al. [5], Epelle et al. [6], and Foroud et al. [7] have highlighted that drag control in shale drilling involves coupled effects of geological, operational, and fluid-related factors. These nonlinear relationships (e.g., the synergistic effect of shale hydration and drilling fluid degradation cannot be accurately described by single numerical simulations) exceed the characterization capabilities of traditional analytical and numerical simulations. Modeling approaches that neglect hierarchical analysis of controlling factors often result in the loss of key parameters during data preprocessing. Moreover, the internal decision-making logic of complex "black-box" algorithms is difficult to manually trace, significantly limiting their credibility in engineering applications.

In terms of data statistics, Zou et al. [8], Bai et al. [9], Zhang et al. [10], and Zhong et al. [11] have pointed out that drilling data exhibit distinct multi-scale, multi-source, and multi-modal characteristics. Spatially, they cover physical parameters from different lithological sections; temporally, they span various operational phases such as drilling and tripping; data sources include real-time instrument measurements, manual intermittent records, and laboratory physical simulations with varying reliability levels. Additionally, structured WOB data often coexist with unstructured data (e.g., cuttings images). Concurrently, limited valid samples per well and significant inter-well variations mean that direct application of big data algorithms may lead to low accuracy and overfitting issues.

Concerning data preprocessing, Zang et al. [12], and Feng et al. [13] have noted that current preprocessing methods often analyze single operational parameters in isolation. They fail to consider the coupling effects of multiple drag reduction techniques (e.g., composite drilling fluids and hydraulic tools) and neglect interference from geological structural undulations and fluctuations in drilling parameters, resulting in severe loss of key feature information. Direct application of intelligent algorithms to drilling data analysis—without adapting to the characteristics of small sample sizes and strong noise—often leads to model prediction errors exceeding 20%, which are far from meeting engineering accuracy requirements.

In summary, existing drag reduction research predominantly focuses on validating the effectiveness of single techniques and exploring their specific control mechanisms. However, it lacks systematic analysis of the coupled effects of multiple processes throughout the entire drilling cycle (design-drilling-completion) and insufficiently considers unique issues such as lithological influences, cuttings bed compaction, and multi-scale/multi-source data characteristics. This leads to ambiguous process prioritization and unclear failure thresholds. Therefore, targeting the Jurassic Lianggaoshan Formation reservoir in the Fuxing Block, this study conducts quantitative evaluation and reliability analysis of synergistic multi-process drag reduction to address engineering challenges such as drag exceeding 50t and WOB transfer difficulties in horizontal sections.

2 Geological Background and Dataset

The Fuxing area is located in the Wanxian synclinorium of the Eastern Sichuan high-steep fold belt. The target reservoir, the Jurassic Lianggaoshan Formation, has a burial depth of 2500-2800m and horizontal section lengths ranging from 1500 to 2500m. The wellbore structure typically adopts a "conductor+two-section" design with standard hole sizes: the conductor isolates the unstable Penglaizhen Formation, while the first section isolates the highly permeable upper-middle part of the Shaximiao Formation. The first section uses a potassium-amine-based drilling fluid system, and the second section employs an OBDF system; the completion method adopts a "dual-toe sliding sleeve+casing" system [14–16].

For the first section isolating the upper Shaximiao: The average total depth (TD) was 5008m, with a long drilling cycle of 69.92 days and a low average ROP of 10.23 m/h. The upper formations are mostly unconsolidated sediments with poor stability, prone to wellbore instability and fluid loss, requiring frequent adjustments to drilling parameters and practices, which significantly impacts efficiency.

For the first section isolating the middle Shaximiao: The average TD was 4750m, with a reduced cycle of 52.11 days and an improved ROP of 13.47m/h. The lithology is more uniform, reducing drilling difficulty.

For the first section isolating the lower Shaximiao: The average TD was 4934m, with the shortest cycle of 48.45 days (despite a slightly lower ROP of 12.45m/h). Based on quantitative metrics, this well design is optimal: its comprehensive drilling efficiency (ROP/cycle=0.257m·h^{-1}·day^{-1}) is 12.3% higher than that of the middle section and 46.8% higher than that of the upper section.

Abnormal drag in the Fuxing area mainly occurs in horizontal wells targeting the Dongyuemiao

and Lianggaoshan formations. High drag in the reservoir section leads to WOB transfer difficulties. Established understandings include: 1) High porosity and permeability of continental shale facilitate the formation of thick filter cakes; 2) Low strength of continental shale and rapid OBDF degradation cause cuttings dispersion; 3) Amphiphilic and strong oil-affinity properties exacerbate cuttings dispersion; 4) Faster pressure transmission compared to marine shale provides conditions for thick filter cake formation; 5) Rapid OBDF degradation results in mud-like cuttings, with filter cake thickness 2-3 times that of marine shale; 6) Compacted cuttings beds are difficult to transport, leading to poor hole cleaning; 7) Differential sticking causes abnormal drag.

This study utilizes field data from 14 wells in the Fuxing Block, focusing on the second drilling phase. A closed-loop methodology of "data integration→model quantification→reliability verification" is adopted for process optimization. The specific workflow is as follows (Figure 1): 1) Preprocess and standardize key factors (drilling fluid properties, well trajectory, engineering parameters) based on theoretical drag formulas and field experience; 2) Construct a hierarchical structure using the AHP model, integrate multiple local linear models to quantify the weights of drilling fluid materials, technical measures, and design optimization, and identify priority factors; 3) Apply the Reliability Analysis model to fit censored field drag data, identify failure thresholds and reliability decay patterns of typical techniques, and ultimately form a theoretically sound and practically feasible drag reduction strategy.

3 Methodology

3.1 Data Preprocessing

Key factors in drag reduction include proper drilling fluid maintenance, the selection of appropriate drag-reduction measures, and optimization of drilling design. In addition to lithology, external factors influencing drag comprise well depth, horizontal section length, reaming time, tripping time, and rate of penetration (ROP). This study focuses on the second section, with geological variations excluded due to the consistency of the target formation. Data preprocessing entails the systematic selection and rigorous definition of variables related to drilling fluid properties, well trajectory, drag during drilling and casing running, and fundamental engineering parameters, as summarized in Data Record Table 1.

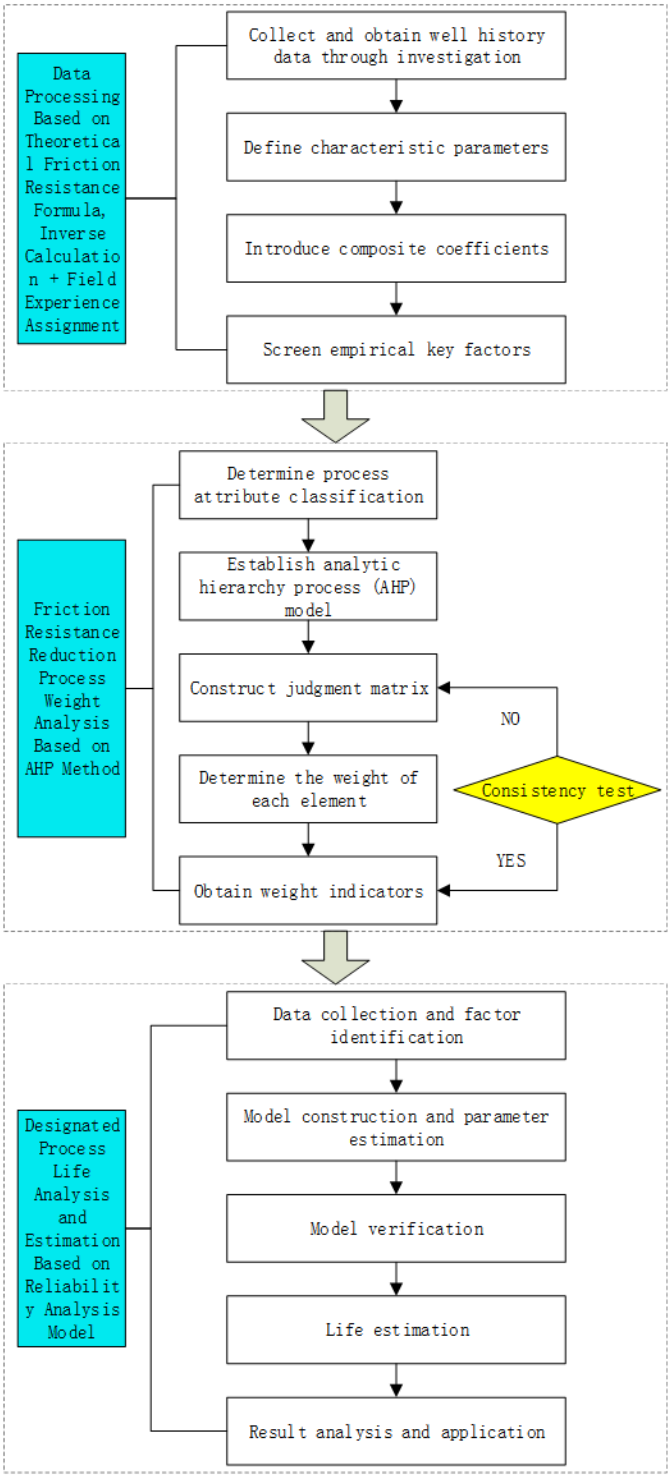

Figure 1. Logic diagram of the research process.

(1) Average Drag Coefficient and Casing Running Drag Index

These two parameters are selected to quantitatively evaluate drag during drilling and casing running operations.

The Average Drag Coefficient covers the entire process of tripping, reaming, and other activities in the second drilling section, reflecting the overall average frictional

Table 1. Pretreatment records of drilled well data.

Well No	Total Drilled Depth, m	Horizontal Section Length, m	Reaming Efficiency of 2nd Spud-in, %	Average ROP of 2nd Spud-in, m/h	Tripping Efficiency, %	Overall Reaming Efficiency, %	Average Friction Coefficient of 2nd Spud-in	Casing Running Method	Casing Running Friction Index	Average Dogleg Severity of 2nd Spud-in, deg/30m	Maximum Dogleg Severity of 2nd Spud-in, deg/30m	Trajectory Smoothness Coefficient of 2nd Spud-in, TSC	Reduction Rate of Lubrication Coefficient of 2nd Spud-in, %	Drilling Fluid Friction Coefficient of 2nd Spud-in, μ	Lubricant Dosage of 2nd Spud-in, t/100m^3
XYL257-4-1HF	5350	2532	10.56	20.81	18.84	7.2	0.25	Conventional	0.46	1.51	5.89	1.14	17.991	0.04499	5.5
XYL12HF	5430	2388	0	11.01	7.08	0	0.31	Rotational Casing Running	0.47	2.06	6.44	0.82	22.122	0.04858	5.0
XYL211-6-1HF	5430	2531	0	14.56	11.69	0	0.37	Conventional	0.57	0.05	0.23	1.19	14.944	0.06124	5.1
XYL231-4-1HF	5513	2532	0	14.58	11.15	0	0.23	Conventional	0.44	0.05	0.25	1.18	25.117	0.04961	5.2
XYL185-6-1HF	5290	2530	0	20.97	9.02	0	0.25	Conventional	0.45	1.23	5.92	1.36	19.053	0.06309	4.2
XYL197-6-1HF	5838	3033	5.76	12.7	3.26	6.25	0.31	Conventional	0.54	2.11	7.19	0.83	21.090	0.04460	4.0
XYL190-6-1HF	5326	2531	2.4	10.27	33.71	1.72	0.27	Conventional	0.38	1.28	8.55	1.46	16.097	0.07026	5.4
XYL186-6-1HF	5320	2535	1.65	15.37	18.26	0.92	0.29	Conventional	0.41	1.32	5.22	1.32	23.068	0.05246	4.6
XYL213-6-1HF	5839	3035	0.77	15.27	14.39	0.36	0.3	Floating Casing Running	0.45	1.35	7.6	1.34	16.965	0.06304	5.3
XYL1006HF	5820	3031	26.28	20	7.6	14.78	0.28	Floating + Rotational Casing Running	0.32	1.54	7.43	1.37	20.093	0.05138	4.6
XYL226-6-1HF	5470	2500	0	14.34	11.42	0	0.31	Conventional	0.38	1.5	7.36	1.15	24.077	0.05326	4.3
XYL198-6-1HF	5290	2531	17.42	18.6	8.48	12.83	0.33	Conventional	0.39	1.59	6.4	1.07	18.036	0.04949	4.0
XYL1003HF	5423	2500	9.1	15.22	9.95	8.32	0.21	Conventional	0.31	1.5	7.41	1.19	22.047	0.06223	4.8
XYL1004HF	5064	2097	5.13	13.03	13.18	3.92	0.26	Conventional	0.42	1.75	5.81	1	23.127	0.04863	4.8

force between the drill string and the wellbore wall [17]. Its calculation formula is:

$$f = \frac{\Sigma_F}{\Sigma_N} \tag{1}$$

where Σ_F represents total frictional force along the drill string; Σ_N represents total normal force acting on the drill string.

The Casing Running Drag Index is a quantitative metric constructed based on the "time-obstruction frequency" composite evaluation method proposed by Wang et al. [18], primarily characterizing casing running efficiency under predetermined footage intervals. Its calculation formula is:

$$MI = \frac{T_a}{T_0} \times Fr_i \tag{2}$$

where T_a represents the actual casing running time; T_0 represents the theoretical casing running time under ideal frictionless conditions; Fr_i represents the frequency of obstructions encountered during casing running.

(2) Dogleg Severity (DLS) and Trajectory Smoothness Coefficient

These parameters quantitatively characterize the complexity, spatial geometry, and frictional implications of the wellbore trajectory, converting qualitative descriptions (e.g., "upward inclination," "downward inclination," "undulating/wavy") in completion reports into objective, measurable metrics.

The DLS is defined in accordance with the Chinese petroleum industry standard SY/T 5435-2012 ("Quality Control Specification for Oil Well Trajectory"), which recommends 30 m as the standard course length for conventional wellbore trajectory curvature evaluation. This selection ensures consistency with industry practice and comparability of trajectory data across the 14 wells. DLS represents the rate of change of both inclination and azimuth angles per unit wellbore length, directly indicating trajectory curvature sharpness [19]. Its calculation formula is:

$$\mathrm{DLS} = \frac{\sqrt{(\Delta\alpha)^2 + (\Delta\theta \cdot \sin\alpha_m)^2}}{L} \times 30 \tag{3}$$

where $\Delta\alpha$ represents the change in inclination angle (°); $\Delta\theta$ signifies the change in azimuth angle (°); α_m denotes the average inclination angle (°); L is the course length (m, 30 meters is adopted in this study).

The Trajectory Smoothness Coefficient (TSC) is a dimensionless parameter characterizing the relative relationship between discrete DLS fluctuations and the average curvature within a wellbore interval. It is defined as the ratio of the standard deviation to the mean of the DLS sequence at consecutive survey stations, effectively quantifying wellpath "smoothness-undulation" characteristics [20]. Its calculation formula is:

$$\mathrm{TSC} = \frac{\sigma_{\mathrm{DLS}}}{\mu_{\mathrm{DLS}}} \tag{4}$$

where σ_{DLS} denotes the standard deviation of the Dogleg Severity (DLS) sequence; μ_{DLS} represents the mean value of the DLS sequence.

(3) Drilling Fluid System Evaluation Parameters

Three key parameters—Lubricity Reduction Rate, Drilling Fluid Friction Coefficient, and Lubricant Dosage—are selected to quantitatively evaluate drilling fluid system selection and performance maintenance.

The Lubricity Reduction Rate is a critical performance indicator, quantifying the variation in drilling fluid lubricity with accumulated footage. It is evaluated in strict accordance with SY/T 6094-1994 ("Evaluation Procedure for Lubricants in Drilling Fluids") under 25°C and atmospheric pressure [21]. Its calculation formula is:

$$R_x = \frac{K_0 - K_1}{K_0} \times 100\% \tag{5}$$

where K_0 represents the lubricity coefficient of the base fluid; K_1 denotes the lubricity coefficient of the drilling fluid after lubricant addition.

Meanwhile, real-time field measurements of the drilling fluid friction coefficient and lubricant dosage are systematically recorded throughout drilling operations, enabling dual-faceted evaluation of fundamental lubricating performance and lubricity maintenance effectiveness.

Based on Table 1, the following conclusions are drawn:

1. Even after data preprocessing, evaluating the influence of certain factors on the Casing Running Drag Index remains challenging. These factors include drilling design parameters (e.g., total well depth, lateral section length), engineering parameters (e.g., reaming efficiency, ROP), trajectory-related factors (e.g., DLS, TSC), and drilling fluid performance parameters (e.g., lubricant dosage, Lubricity

Reduction Rate). 2. Field experience from design optimization shows that as casing setting depth increases, the ROP of the first spud-in section tends to decrease, leading to a corresponding extension of the drilling cycle. Specifically, when casing is set to seal the upper part of the Shaximiao Formation and fully isolate the formation, the ROP decreases from 15.93m/h to 12.27m/h, and the drilling cycle increases from 6.5 days to 13.38 days.

3.2 Analytical Hierarchy Process Model Analysis

The AHP essentially solves multi-objective decision-making problems. Its core principle involves clustering abstract factors (manually or mathematically), integrating them with problem logic into a hierarchical structure (goal level, criterion level, alternative level), and quantifying factor weights through matrix construction and pairwise comparison of inter-factor relationships [22]. In this study: The goal level is defined as drag reduction effectiveness. Based on 14-well field data from preprocessing, drag reduction processes are clustered into three criterion-level aspects (drilling fluid materials, technical measures, design optimization), further subdivided into 12 items to form two criterion levels. The alternative level is constructed based on three evaluation dimensions: economic cost, time efficiency, and durability.

1. Determine the goal of reducing friction resistance effectiveness and construct the hierarchical structure model.

2. Based on the comprehensive correlation degree calculation results (of sequence B relative to A, C relative to B, D relative to C) and engineering experience, perform pairwise comparison scoring to determine the scores of lower levels relative to the upper level. Due to the engineering complexity of this model, two criterion levels are established, distinguishing between different alternatives for drilling fluid materials, technical measures, and design optimization. As the relative importance of each factor varies under the decision-maker's criteria, the scale of numbers 1-9 and their reciprocals are used to define the judgment matrix.

3. Hierarchical synthesis calculation and consistency check. Use Equation (6) to calculate the Consistency Index (CI):

$$CI = \frac{\lambda_{\max} - n}{n - 1} \tag{6}$$

where $\lambda_{\max}$ the largest eigenvalue of the judgment matrix, and n is the order of the matrix.

Use Equation (7) to calculate the Consistency Ratio (CR):

$$CR = \frac{CI}{RI} \tag{7}$$

where CI is the Consistency Index, and RI is the Random Consistency Index.

When $CR < 0.10$, it indicates passing the consistency check; otherwise, the consistency is unsatisfactory.

4. Calculate the weight vector using the geometric mean method (taking the nth root of the continuous product of n variable values). The geometric mean is used to find the development speed of the prediction target:

$$W_i = \frac{\left(\prod_{j=1}^{n} a_{ij}\right)^{\frac{1}{n}}}{\sum_{i=1}^{n}\left(\prod_{j=1}^{n} a_{ij}\right)^{\frac{1}{n}}} \quad i = 1, 2, 3, \ldots, n \tag{8}$$

A structural model diagram for determining the effectiveness of friction reduction methods is illustrated (Figure 2). For convenience in matrix construction, the goal level is labeled A, the criterion levels are labeled B and C, and the alternative level is labeled D. The calculation process is shown in Figure 2.

In the judgment matrix for the goal of reducing friction resistance, mud performance and technical measures are considered equally important. However, design optimization is more important. Thus, the weight ratio for Mud Performance: Design Optimization is set to 1:3. As technical measures offer greater adjustment flexibility, the weight ratio for Technical Measures / Design Optimization is set to 1/2.

A	$B1$	$B2$	$B3$
$B1$	1	1	1/3
$B2$		1	1/2
$B3$			1

(9)

Weight vector $W = (0.2098, 0.2402, 0.5499)$; $CR = 0.0176$

For drilling fluid materials, the combination of glass beads (¥12,000/ton) + super graphite (¥8,000/ton) is commonly used as a lubrication method, demonstrating optimal time efficiency, effect

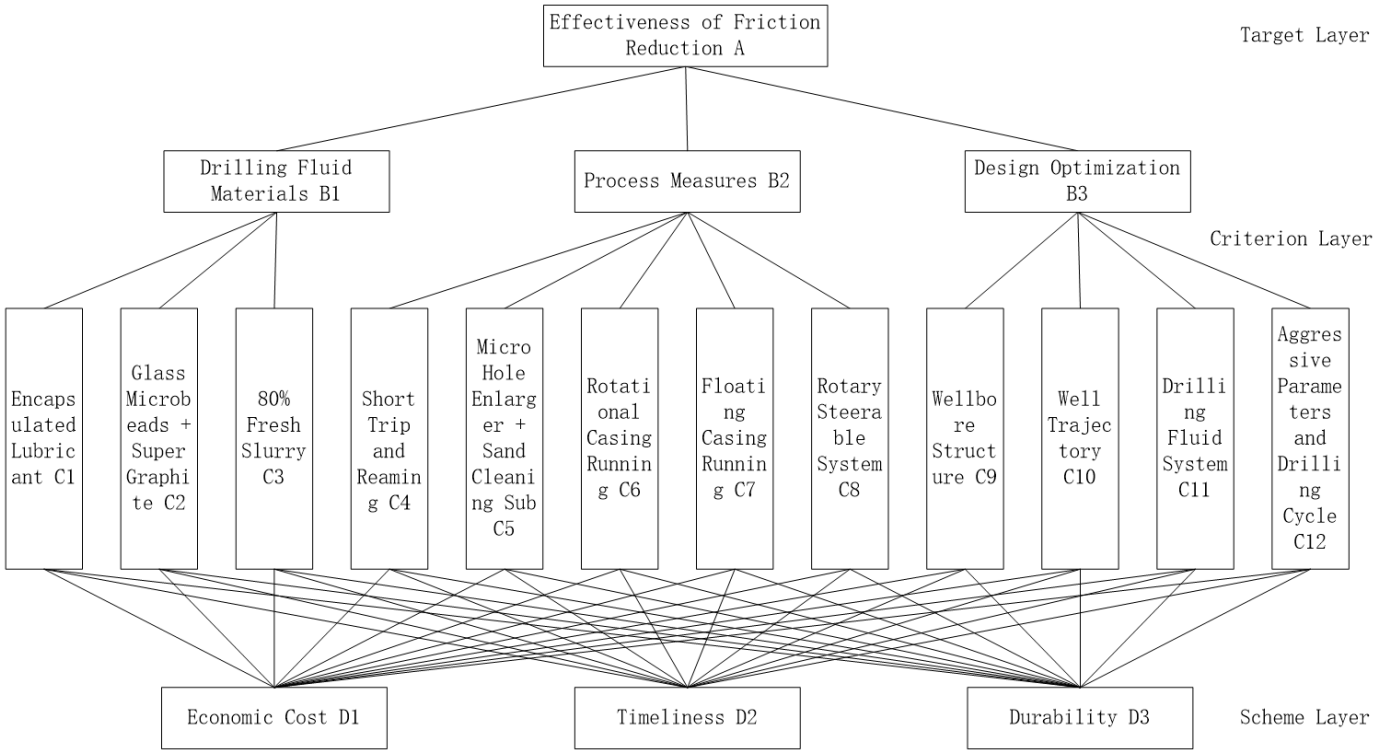

Figure 2. Schematic diagram of the structural model.

durability, and economic cost. Using encapsulated lubricant (¥20,000/ton) at a concentration of 2% only shows significant effect within 100 m of drilling immediately after addition, after which the friction resistance increases significantly. In Well XY L1006HF, when the dosage was increased to 4% at 4550 m, the pickup and slack-off friction resistances were 40 t and 22 t respectively, indicating no reduction. While using 80% new mud throughout the well (¥10,000/m^3), costing approximately ¥1.456 million for a ϕ215.9 mm hole with 5000 m volume offers better durability, it requires mixing time and incurs higher economic costs.

$B1$	$C1$	$C2$	$C3$
$C1$	1	1/3	3
$C2$		1	5
$C3$			1

(10)

Weight vector $W = (0.2583,\ 0.6370,\ 0.1047)$; $CR = 0.0370$

$C1$	$D1$	$D2$	$D3$
$D1$	1	1/3	2
$D2$		1	4
$D3$			1

(11)

Weight vector $W = (0.2385,\ 0.6250,\ 0.1365)$; $CR = 0.0176$

$C2$	$D1$	$D2$	$D3$
$D1$	1	1/2	1/6
$D2$		1	1/5
$D3$			1

(12)

Weight vector $W = (0.1020,\ 0.1721,\ 0.7258)$; $CR = 0.0279$

$C3$	$D1$	$D2$	$D3$
$D1$	1	3	1/2
$D2$		1	1/3
$D3$			1

(13)

Weight vector $W = (0.3325,\ 0.1396,\ 0.5278)$; $CR = 0.0516$

For technical measures, during the drilling process, differentiated reaming (no cost) is performed based on friction conditions, using a micro-reamer + sand trap sub to enhance cuttings transport (no cost), and using rotary steerable systems to smooth the borehole trajectory (80,000/day). During casing running, rotating casing and floating casing techniques are used to improve completion efficiency. However, the rotating casing process requires enhanced casing rigidity, increasing casing and operational costs (100,000–300,000/well) but can improve completion efficiency (saving 120,000/day). Floating casing using float collars and nitrogen injection increases technical

costs (20,000–80,000/well) but also improves completion efficiency (saving 120,000/day).

$B2$	$C4$	$C5$	$C6$	$C7$	$C8$
$C4$	1	1/2	2	2	3
$C5$		1	4	3	1/2
$C6$			1	1/3	1/4
$C7$				1	1/3
$C8$					1

(14)

Weight vector $W = (0.1707,\ 0.2659,\ 0.0668,\ 0.1112,\ 0.3854)$; $CR = 0.0598$

$C4$	$D1$	$D2$	$D3$
$D1$	1	1	3
$D2$		1	1/2
$D3$			1

(15)

Weight vector $W = (0.5816,\ 0.3090,\ 0.1095)$; $CR = 0.0036$

$C5$	$D1$	$D2$	$D3$
$D1$	1	1/3	1/4
$D2$		1	1/3
$D3$			1

(16)

Weight vector $W = (0.6144,\ 0.1172,\ 0.2684)$; $CR = 0.0707$

$C6$	$D1$	$D2$	$D3$
$D1$	1	1/5	1/3
$D2$		1	3
$D3$			1

(17)

Weight vector $W = (0.1047,\ 0.6370,\ 0.2583)$; $CR = 0.0370$

$C7$	$D1$	$D2$	$D3$
$D1$	1	1/3	1/3
$D2$		1	2
$D3$			1

(18)

Weight vector $W = (0.1396,\ 0.5278,\ 0.3325)$; $CR = 0.0516$

$C8$	$D1$	$D2$	$D3$
$D1$	1	1/2	1/2
$D2$		1	2
$D3$			1

(19)

Weight vector $W = (0.1958,\ 0.4934,\ 0.3108)$; $CR = 0.0516$

For design optimization, it typically focuses on the wellbore structure, borehole trajectory, drilling fluid system, aggressive parameters, and drilling cycle. For wellbore structure, optimization involves the regional distribution of the isolation depth for the high-permeability zone in the Shaximiao Formation in the second spud. For borehole trajectory, smoothing optimization is performed for the four-section trajectory design. The lateral section is designed with an upward/downward inclination based on reservoir undulations to avoid wavy patterns. For the drilling fluid system, adjustments are made to the performance of synthetic-based mud and oil-based mud used by Zhongyuan Engineering Company and Jianghan Engineering Company in the second spud. For aggressive parameters and drilling cycle, parameters are intensified to increase the ROP and shorten the drilling cycle as much as possible without causing inefficiencies such as buckling, based on different Bottom Hole Assemblies.

$B3$	$C9$	$C10$	$C11$	$C12$
$C9$	1	1/5	1/4	1/3
$C10$		1	2	3
$C11$			1	2
$C12$				1

(20)

Weight vector $W = (0.0729,\ 0.4729,\ 0.2844,\ 0.1699)$; $CR = 0.0191$

$C9$	$D1$	$D2$	$D3$
$D1$	1	5	3
$D2$		1	1/3
$D3$			1

(21)

Weight vector $W = (0.6370,\ 0.1047,\ 0.2583)$; $CR = 0.0370$

$C10$	$D1$	$D2$	$D3$
$D1$	1	3	2
$D2$		1	1
$D3$			1

(22)

Weight vector $W = (0.5499,\ 0.2098,\ 0.2402)$; $CR = 0.0176$

$C11$	$D1$	$D2$	$D3$
$D1$	1	5	4
$D2$		1	2
$D3$			1

(23)

Weight vector $W = (0.6870,\ 0.1865,\ 0.1265)$; $CR = 0.0904$

$C12$	$D1$	$D2$	$D3$
$D1$	1	3	2
$D2$		1	1/2
$D3$			1

(24)

Weight vector $W = (0.5396,\ 0.1634,\ 0.2970)$; $CR = 0.0088$

All calculated CR values are less than 0.1, passing the consistency check. Furthermore, the weight matrix W of the criteria elements for different alternatives is multiplied by the relative weight matrix W of the criteria elements, respectively, to obtain the weights for the criterion level and the alternative level (Figure 3).

The calculations lead to the following conclusions: The macro-level criterion weight ranking is B3 > B2 > B1, with the weight of B3 being significantly greater than B2 and B1. The micro-level detailed alternative weight ranking is C10 > C11 > C2 > C12 > C8 > C5 > C1 > C4 > C9 > C7 > C3 > C6, with the weight of C10 being significantly greater than other factors. The weights of C11 and C2, C12 and C8, C4 and C9, C7 and C3 are relatively close. The alternative level weight ranking is D1 > D3 > D2.

3.3 Reliability Analysis Model or Process Capability Analysis

Based on AHP results (B3 > B2 > B1), source design optimization meets the multi-dimensional requirements of economy, time efficiency, and durability. However, on-site drag reduction process selection is a composite task requiring multi-perspective optimization. This study selected wells with multi-process or high-weight typical process applications, collected statistics on relative drag versus drilling/casing running lengths, and used the Reliability Analysis model to analyze drag reliability distribution under different process combinations. The model calculates reliability, characteristic life, and failure rate of each process within specific drilling/casing length intervals (with drag $\leq$ threshold), quantifying process stability and effective duration in drag control. This clarifies the inhibitory effect and applicable well sections of high-weight processes in practical production, providing data support for precise on-site process selection and combined application.

The Reliability Analysis model uses reliability as the evaluation indicator. Focusing on "drag data per 100 m", this study correlates drag values of case wells (with different processes) with "drilling length-drag" and imports data into Minitab for reliability distribution fitting [23]. Calculation Steps:

(1) Data Screening. According to the requirements of the Distribution Analysis with Arbitrary Censoring module, input up to 50 columns of sample data containing start times in the initial and end variables. The start time in this column depends on the data censoring method. Input the column containing the failure mode. Use the failure mode column to represent right-censored observations.

(2) Data Fitting and Goodness-of-Fit Test. The failure mode data column may follow models such as the Weibull distribution, Exponential distribution, Extreme value distribution, and Normal distribution. Goodness-of-fit tests for the entire data column are typically performed using Maximum Likelihood, Chi-Square test, and Least Squares functions. The Anderson-Darling test was selected for calculation here:

$$A^2 = -n - \frac{1}{n}\sum_{i=1}^{n}(2i-1)\left[\ln F_0(x_i) + \ln\left(1 - F_0(x_{n-i+1})\right)\right] \tag{25}$$

where $F_0(x_i)$ is the value of the theoretical distribution function at the i-th ordered statistic; $F_0(x_{n-i+1})$ is the value of the theoretical distribution function at the $n-i+1$-th ordered statistic. In practical applications, Minitab software directly computes and reports the test statistic value based on the above formula.

(3) Hypothesis Testing and Reliability Calculation.

The two-parameter Weibull distribution is often preferred in common calculations. Using the Weibull distribution as an example, the failure distribution function $F(t)$ and reliability function $R(t)$ for the two-parameter Weibull distribution are:

$$F(t) = 1 - \exp\left[-\left(\frac{t-\gamma}{\eta}\right)^{\beta}\right] \tag{26}$$

$$R(t) = \exp\left[-\left(\frac{t-\gamma}{\eta}\right)^{\beta}\right] \tag{26}$$

where η is the scale parameter; β is the shape parameter. γ is the threshold parameter.

Statistics and Calibration:

(1) Well XY L1006HF represents the application of encapsulated lubricant (C1), glass beads + super graphite (C2), and 80% new mud (C3).

(2) Well XY L211-6-1HF represents the application of rotary steerable system (C8) and micro-reamer + sand trap sub (C5).

(3) Well XY L213-6-1HF represents the application of floating casing technique (C7).

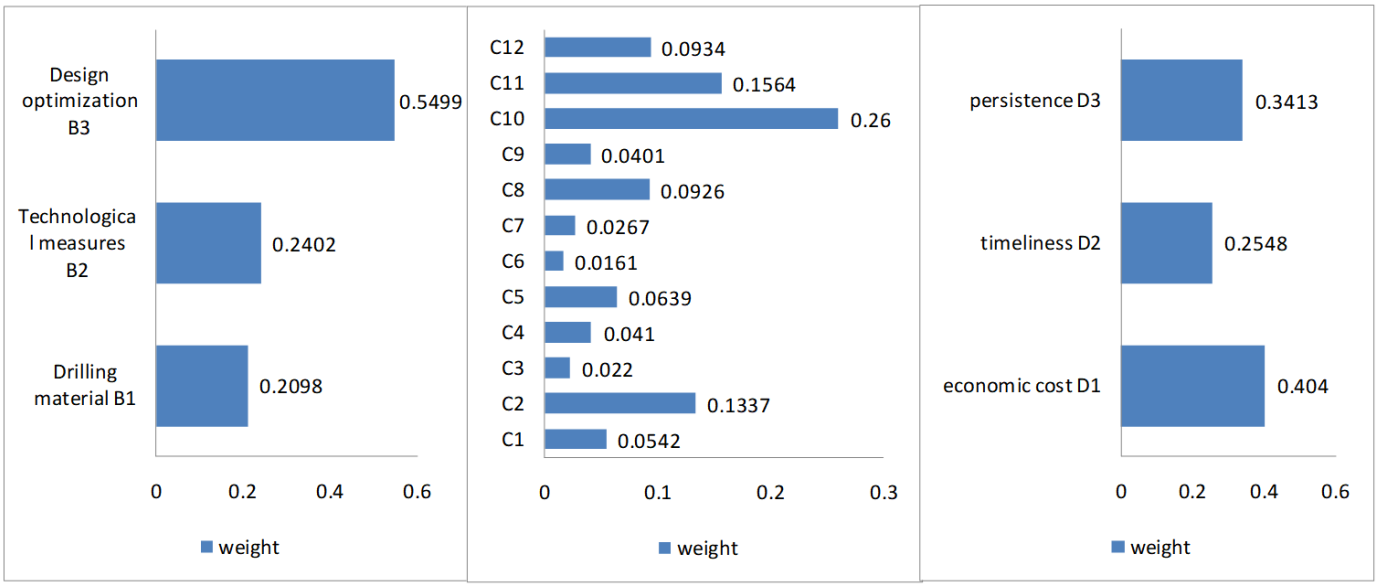

Figure 3. Criterion-level and alternative-level weights obtained from the Analytic Hierarchy Process (AHP) analysis.

(4) Well XY L197-6-1HF represents the application of borehole trajectory optimization (C10) and drilling fluid system optimization (C11).

Wellbore structure (C9) was not analyzed separately due to fixed drilling design requirements (no comparable single-well samples with different wellbore structures). Short-trip reaming (C4) and aggressive parameters & drilling cycle (C12) were not compared with differentiated single-well samples, as their implementation was consistent across all wells. Based on engineering experience, wells with high ROP and short drilling cycles generally exhibit high drag and require separate short-trip reaming.

Drag data during horizontal section circulation runs for the four wells were statistically analyzed. Drag $\leq$ 50t was calibrated as process effectiveness, and "Unable to test" data were treated as right-censored observations (consistent with engineering reliability study practices [24], as these data indicate drag exceeded the measurable threshold but process failure was not directly observed). Reliability analysis under arbitrary censoring was performed (Tables 2, 3, 4 and 5).

Parameter distribution analysis was performed on the circulation friction resistance data for Wells XYL1006HF, XYL211-6-1HF, XYL213-6-1HF, and XYL197-6-1HF using the best-fit distribution models identified above. The results are as follows (Figure 4).

Well XYL1006HF: Estimated location parameter = 72.6320, scale parameter = 29.7297, log-likelihood = −76.749 (reasonable model accuracy). Data points deviate slightly from the Smallest Extreme Value distribution curve, possibly due to limited drag reduction effect of encapsulated lubricant and unclear coupling effects of the combined processes. Fitted average pick-up drag = 55.47t; survival probability (drag $\leq$ 50t) decreases with increasing drag: 50% effectiveness at 61.74t, 10% at 97.43t. Field records: Drag increased by 2–4t per 100m after entering the horizontal section; adding 2.5% encapsulated lubricant at 4260m did not reduce pick-up drag (36t, only

Table 2. Friction Resistance vs. Horizontal Section Length Data for Well XY L1006HF.

Drilling Length, m	Pick-up Friction, t	Drilling Length, m	Pick-up Friction, t	Drilling Length, m	Pick-up Friction, t
100	10	1100	40	2100	65
200	12	1200	42	2200	67
300	14	1300	46	2300	69
400	18	1400	52	2400	71
500	20	1500	55	2500	73
600	24	1600	57	2600	75
700	28	1700	59	2700	Unable to test
800	32	1800	60	2800	Unable to test
900	36	1900	62	2900	Unable to test
1000	38	2000	64	3000	Unable to test

Table 3. Friction Resistance vs. Horizontal Section Length Data for Well XY L211-6-1HF.

Drilling Length, m	Pick-up Friction, t	Drilling Length, m	Pick-up Friction, t	Drilling Length, m	Pick-up Friction, t
100	18	1100	58	2100	Unable to test
200	20	1200	62	2200	Unable to test
300	22	1300	65	2300	Unable to test
400	26	1400	70	2400	Unable to test
500	28	1500	75	2500	Unable to test
600	32	1600	Unable to test	2600	Unable to test
700	36	1700	Unable to test	2700	Unable to test
800	42	1800	Unable to test	2800	Unable to test
900	50	1900	Unable to test	2900	Unable to test
1000	55	2000	Unable to test	3000	Unable to test

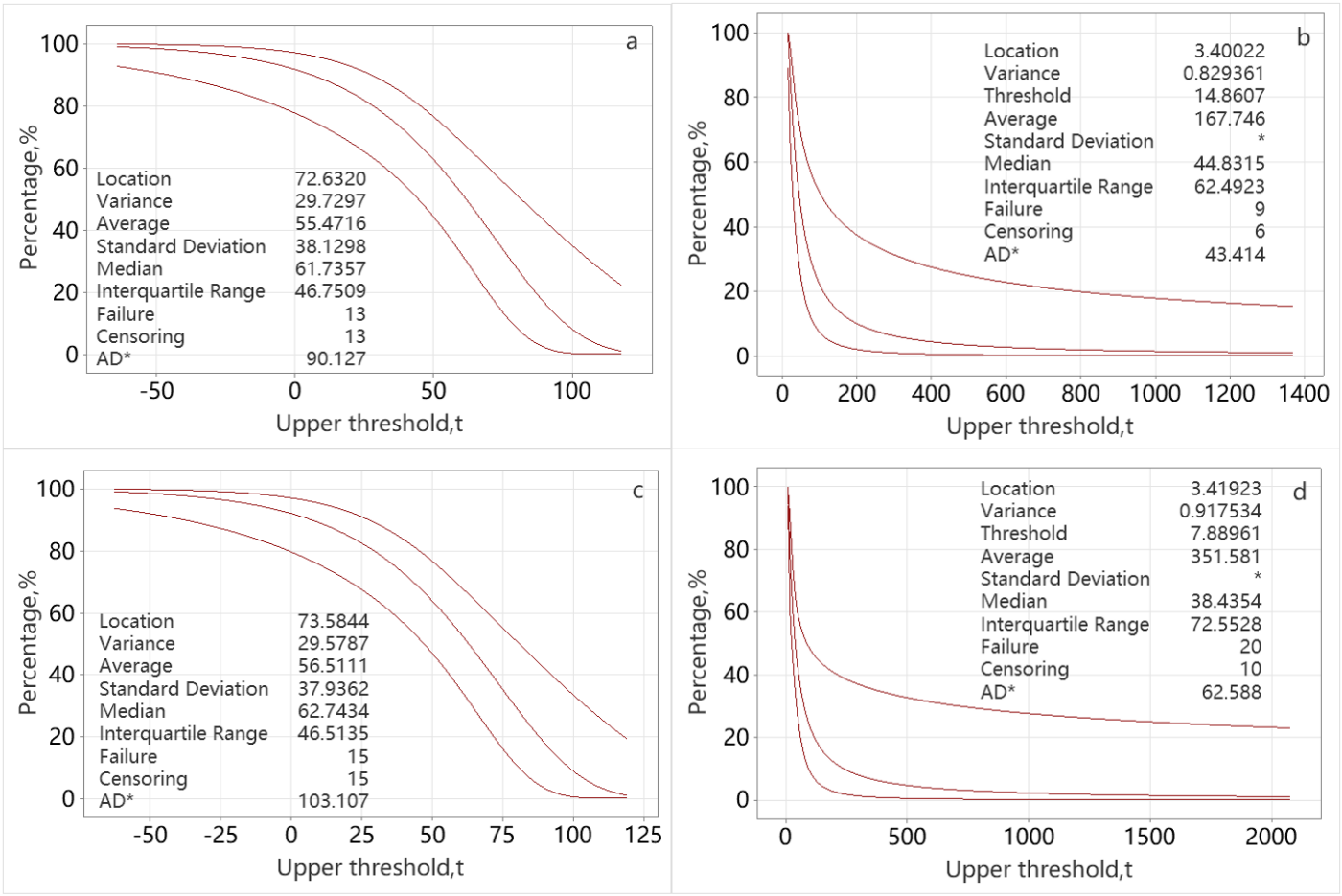

*Note: a = Well XY L1006HF; b = Well XY L211-6-1HF; c = Well XY L213-6-1HF; d = Well XY L197-6-1HF

Figure 4. Survival curves showing the reliability (probability of pick-up drag $\leq 50\,t$) as a function of increasing friction force for four representative wells employing different drag reduction processes.

slack-off drag decreased by 8t); increasing dosage to 4% at 4550m still showed no drag reduction. Conclusion: Encapsulated lubricant requires a specific concentration, with significant immediate effects after addition but gradual consumption during horizontal drilling; timely replenishment is necessary to avoid sharp drag increases.

Well XYL211-6-1HF: Estimated location parameter = 3.4002, scale parameter = 0.8293, log-likelihood = −43.318 (good fit with Log-Logistic distribution). Fitted average pick-up drag = 167.746t; 50% effectiveness at 44.8315t, 10% at 200.260t. Despite using a rotary steerable system (TSC = 1.19), no reaming was performed for the 2500m horizontal section (ROP = 14.56m/h), leading to multiple circulation run obstacles. Field records: A high-density biomass synthetic-based drilling fluid (1.64–1.66g/cm^3) was used; drag and torque increased significantly after the horizontal section exceeded 1500m, with rib sticking observed; tool vibration risks exist when drilling through sand-shale interbeds in the build-up section.

Table 4. Casing Running Friction Resistance vs. Horizontal Section Length Data for Well XY L213-6-1HF.

Drilling Length, m	Pick-up Friction, t	Drilling Length, m	Pick-up Friction, t	Drilling Length, m	Pick-up Friction, t
100	18	1100	32	2100	63
200	19	1200	36	2200	63
300	20	1300	42	2300	64
400	21	1400	45	2400	66
500	22	1500	47	2500	69
600	23	1600	51	2600	72
700	25	1700	53	2700	73
800	27	1800	55	2800	74
900	29	1900	57	2900	75
1000	30	2000	60	3000	75

Goodness-of-fit for the friction resistance data series was determined via the Chi-Square test, screening for the best distribution model (Table 6).

Well XYL213-6-1HF: Estimated location parameter = 73.5844, scale parameter = 29.5787, log-likelihood

Table 5. Friction Resistance vs. Horizontal Section Length Data for Well XY L197-6-1HF.

Drilling Length, m	Pick-up Friction, t	Drilling Length, m	Pick-up Friction, t	Drilling Length, m	Pick-up Friction, t
100	8	1100	29	2100	51
200	10	1200	31	2200	55
300	12	1300	34	2300	56
400	12	1400	35	2400	58
500	14	1500	36	2500	60
600	16	1600	40	2600	62
700	18	1700	44	2700	65
800	20	1800	45	2800	66
900	24	1900	46	2900	69
1000	27	2000	48	3000	71

Table 6. Conclusions on the Best distribution model.

Well	Anderson-Darling Statistic	Best Distribution
XY L1006HF	0.926	Minimum class value
XY L211-6-1HF	1.146	Parametric Log-Logistic
XY L213-6-1HF	1.238	Minimum class value
XY L197-6-1HF	0.858	Parametric Log-Logistic

$= -88.382$ (good fit with Smallest Extreme Value distribution). Floating casing achieved an average drag of $\sim$ 56.51t; 50% effectiveness at 62.74t, 10% at 98.25t. The technique shows good drag control under conventional conditions and stronger engineering applicability than conventional casing running, suitable for wells with high circulation drag and poor borehole trajectory. Field records: 3035m horizontal section (TSC $=$ 1.34); 3.77 days of pumping while back-reaming, recovering 1m^3 of $4 \times 3 \times 0.5$cm fragments and 1.5m^3 of cuttings. Recommendation: Floating casing is only suitable for extremely challenging well conditions, considering cost factors.

Well XYL197-6-1HF: Low TSC (0.83), $>$ 80% new mud usage, and low-density drilling fluid (1.4–1.65g/cm^3) were selected to evaluate trajectory/drilling fluid optimization. Fitted average pick-up drag $=$ 351.581t; 50% effectiveness at 38.4354t, 10% at 237.241t. The oil-based mud (low viscosity/gel strength, fluid loss, and solids content) combined with 3000–7000 mesh microcrystalline nanomaterials (sealing formation micropores) effectively reduced differential pressure sticking. Field verification: Successfully handled 2 lost circulation events and controlled drag during sidetracking at 3700m.

Consistent with Yu et al. [25], low trajectory smoothness increases drill string-wellbore contact complexity, while optimized low-density drilling fluid + nanomaterials mitigates drag by reducing overbalance pressure and filter cake thickness. High new mud percentage ensures lubricant stability, forming a persistent drag reduction barrier. This "drilling fluid compensation for trajectory deficiencies" provides a novel approach for drag control in continental shale horizontal wells with constrained trajectory optimization.

4 Results and Discussion

4.1 Key Findings from Mathematical Modeling

Source design optimization significantly reduces drilling difficulty, providing systematic support for process and drilling fluid system adjustments to lower drag. Design-phase priorities include borehole trajectory optimization, appropriate drilling fluid system selection, and the recommended use of the glass beads+super graphite drag reducer formulation.

Drilling-phase aggressive parameter implementation requires rotary steerable tools to minimize the drilling cycle while ensuring trajectory smoothness. Subsequent measures (micro-reamer+sand trap sub [C5], encapsulated lubricant [C1]) have weights 0.02 lower than C8 (rotary steerable system), contributing less to drag reduction. Field experiments confirm: The micro-reamer+sand trap sub improves borehole cleaning only at sufficient flow rates; encapsulated lubricant is effective only within 100 m post-addition.

Completion-phase floating casing technique adoption depends on cost and circulation drag, tentatively recommended for Fuxing Block wells with horizontal sections >2500 m and TSC >1.3 (high wellbore tortuosity).

Alternative-level sub-item weights show no significant differences; drag reduction process selection should prioritize economic cost, choosing consistently effective options within drilling investment constraints.

4.2 Engineering Guidelines

4.2.1 Drilling Engineering

Adhere to the principle of "precise drag control, dynamic drilling fluid performance optimization, and efficient adaptation to complex conditions." Closely monitor pick-up drag data; synergistically regulate drilling engineering and the drilling fluid system to lay the foundation for safe and efficient drilling, enabling targeted responses to complex well conditions and completion challenges.

Drag Monitoring and Alert: Based on Well XYL1006HF calculations, when drag approaches 61.74t (the median failure threshold of encapsulated lubricant), increase field inspections, check drill string wear and

borehole cleanliness, and prepare to replace lubricants or adjust drilling parameters (e.g., WOB, RPM) to prevent complete lubricant failure.

Real-time Trajectory Correction: Use MWD data to monitor DLS in real-time, ensuring $\leq 3°/30$m in the build-up section and $\leq 2°/30$m in the horizontal section to avoid localized drag spikes from abrupt trajectory changes. For deviations, prefer "small-angle, gradual correction" to minimize wellbore disturbance. If directional drilling is difficult after cleaning the cement plug in the second spud, switch to a rotary steerable system (where wellbore stability and downhole safety permit) to increase ROP and shorten the second spud cycle.

Dynamic Parameter Adaptation: Adjust parameters phase-wise. In the build-up section: Use "medium WOB (12–14t), high RPM (80–90rpm), high flow rate (35–40L/s)" to balance ROP and drag control. In the horizontal section: Use "high WOB (16–18t), high RPM (80–90rpm), high flow rate (35–40L/s)" to reduce static contact time and mitigate drag accumulation.

4.2.2 *Drilling Fluid Optimization*

Closely monitor drilling fluid properties and promptly optimize the formulation to inhibit excessive filter cake formation and cuttings dispersion. Dynamically adjust the concentration and replenishment frequency of drag-reducing materials (e.g., encapsulated lubricant) based on horizontal section length to enhance long-term effectiveness and alleviate weight transfer issues.

Sealing and Wall-Building Capacity: Reduce fluid loss (HTHP/110°C <1ml) and optimize bridging agent particle size grading (3000-7500mesh) to prevent thick, weak filter cake formation. Seal formation micropores to reduce the compaction effect of overbalance pressure on the drill string.

Lubricity: Use encapsulated lubricants (pressurized and encapsulated special lubricating materials) for localized, high-concentration, targeted lubrication. Prefer intelligent encapsulated lubricants with a concentration of ˜4% and >80% of particles <30μm to reduce drag.

Drilling Fluid Purification: Use shale shakers with at least 300-mesh screens; operate high-speed centrifugers at >2800 rpm for 12-16 hours/day.

Cuttings Dispersion Control: Enhance inhibition by increasing calcium chloride content to 28%-30% (supported by Lianggaoshan Formation core tests: this concentration reduces shale linear expansion rate by 62% compared to fresh water, effectively inhibiting clay hydration). Introduce new oil-based flocculants to reduce cuttings dispersion; monitor particle size distribution using a particle size analyzer.

Regular Wellbore Cleaning: Use new mud and fibers for high-flow-rate wellbore cleaning to reduce solids content, remove thick, weak filter cake from the wellbore wall, wash off cuttings adhering to the filter cake, and flush the cuttings bed.

4.2.3 *Complex Well Condition Handling and Completion*

For wells with a high incidence of complex faults, excessively pursuing high-smoothness trajectories is unnecessary. A stable downhole drag control system can be established by directionally adjusting drilling fluid density, rheological parameters, and sealing capacity—particularly suitable for drag management during complex operations such as lost circulation handling and sidetracking.

Formation-Specific Fluid Management: In the Upper Shaximiao Formation and above, maintain K^+ concentration ≥ 20000 mg/L, ensuring the drilling fluid contains 1% ultra-fine calcium carbonate and 1% nano-calcium. Before entering the Lower Shaximiao Formation, gradually add 2–3% KCl to raise $K^+ > 25000$ mg/L, while increasing asphalt content to 3%, ultra-fine calcium to 2%, and nano-calcium to 2%, controlling API fluid loss within 5 ml to prevent formation collapse. Enhance inhibition for upper formations and set appropriate mud density to ensure wellbore stability.

Casing Running Method Selection: For wells with a horizontal section end drag factor > 0.4, consider increasing the casing grade, using ball-type centralizers in the horizontal section, and employing a rotating casing system to ensure the safety of sealing components during casing setting. For floating casing applications, appropriately reduce the toe sleeve outer diameter and use a "rotating guide shoe + float collar" combination; precisely adjust the float collar position based on well depth and trajectory.

4.3 Novelty, Advantages, and Limitations

Novelty: Proposed the "Casing Running Drag Index" by combining theoretical drag formula back-calculation and field experience assignment, overcoming the limitation of existing metrics (only considering running time) in comprehensively evaluating casing running efficiency under complex wellbore conditions.

Integrated the AHP and Reliability Analysis models to establish a "weight-oriented" process optimization logic, realizing full-chain drag reduction process demonstration from "contributing factor ranking" to "performance boundary definition" to "engineering adaptation optimization."

Advantages of the Composite Model: Compared with single models, the "AHP + Reliability Analysis" approach offers unique advantages: AHP alone only ranks factor importance without considering performance stability, while Reliability Analysis alone only identifies failure thresholds without prioritizing processes. The composite model achieves cross-scale data fusion/alignment, hierarchical optimization and isolation of controlling factors, and back-calculation under optimal objectives and constraints, making it closer to field engineering practice.

Limitations: The analysis is based on data from 14 wells in the Fuxing Block, not covering the full range of well conditions across different structural zones and horizontal section lengths (e.g., <2000 m, 2000-3000 m, >3000 m). Insufficient data exist to fit a drag prediction formula and process weight correction model applicable to the entire block.

The interaction effects of drilling fluid properties (e.g., viscosity, fluid loss), lithology changes (sand-shale interbed ratio), and tool parameters (BHA, RSS RPM, centralizer spacing) on drag control effectiveness have not been investigated through multi-factor orthogonal experiments or systematic statistical analysis; relevant coupling mechanisms require further validation.

Although the drilling process is divided into three stages (design, drilling, completion) for optimization, research on the specific geological conditions of the Dongyuemiao and Lianggaoshan shale formations is not in-depth, and the optimal thresholds for process switching between stages remain unclear.

5 Conclusions

Focusing on the Fuxing Block in southeastern Sichuan, this study decomposed the complex nonlinear drag reduction problem into a small-sample linear problem. Through systematic collection of field engineering data on multiple drag reduction processes and coupled AHP-Reliability Analysis model solution, local linear approximation was achieved, providing engineered support for the nonlinear drag reduction problem and refining its modeling and evaluation framework.

(1) Pick-up drag during horizontal section drilling exceeded 50t in 12 of 14 wells (85.7%). Encapsulated lubricant alone was effective only within 100 m post-addition, with a failure threshold drag of 61.74t. During completion, floating casing technology enhanced drag control reliability for wells with horizontal sections > 2500m. Optimizing drilling fluid density to 1.4–1.65g/cm^3 and meeting the Lubricity Reduction Rate standard achieved a maximum ROP of 20.97m/h and a minimum drilling cycle of 48.45 days.

(2) AHP modeling indicated design optimization (weight 0.5499) contributed the most to drag reduction, with borehole trajectory optimization (C10) and drilling fluid system selection (C11) having the highest weights in this category. The glass beads + super graphite combined lubrication process (weight 0.6370) demonstrated superior cost and performance advantages compared to other lubrication options.

(3) Future research should expand the sample size to cover well conditions across different structural zones of the Fuxing Block (including horizontal sections $<$ 2000m and $>$ 3000m) to develop a block-wide drag prediction formula. Concurrently, multi-factor orthogonal experiments are needed to investigate the interactions of drilling fluid properties, lithological variations, and tool parameters, clarifying coupling mechanisms. Further refine research considering differences between the Dongyuemiao and Lianggaoshan formations, involving detailed design, precise drilling fluid performance control, and quantification of parameter adjustment thresholds for each operational stage.

Data Availability Statement

Data will be made available on request.

Funding

This work was supported by the China Petrochemical Shale Gas “Ten Dragons” Science and Technology Research Project under Grant P18051.

Conflicts of Interest

Yunfeng Hu is affiliated with the Technology Development Department, Sinopec Jianghan Engineering Company, Wuhan 430024, China; Ye Yang is affiliated with the Drilling Company No.1 of Sinopec Jianghan Petroleum Engineering Co., Ltd., Qianjiang 433123, China. The authors declare that these affiliations had no influence on the study design,

data collection, analysis, interpretation, or the decision to publish, and that no other competing interests exist.

AI Use Statement

The authors declare that no generative AI was used in the preparation of this manuscript.

Ethical Approval and Consent to Participate

Not applicable.

References

[1] Wang, B., Sun, J., Shen, F., Li, W., & Zhang, W. (2020). Mechanism of wellbore instability in continental shale gas horizontal sections and its water-based drilling fluid countermeasures. *Natural Gas Industry B, 7*(6), 680-688. [CrossRef]

[2] Lv, J., Zhang, F., & An, M. (2025). Frictional Stability of Deep Longmaxi Shale in the Southern Sichuan Basin: In Situ Temperature and Pressure Effects on Injection-Induced Seismicity. *Rock Mechanics and Rock Engineering, 58*(9), 10199-10214. [CrossRef]

[3] Zhang, L., He, X., Li, X., Li, K., He, J., Zhang, Z., ... & Liu, W. (2022). Shale gas exploration and development in the Sichuan Basin: Progress, challenge and countermeasures. *Natural Gas Industry B, 9*(2), 176-186. [CrossRef]

[4] Swai, R. E. (2020). A review of molecular dynamics simulations in the designing of effective shale inhibitors: application for drilling with water-based drilling fluids. *Journal of Petroleum Exploration and Production Technology, 10*(8), 3515-3532. [CrossRef]

[5] Wang, X., Ni, H., Shor, R., & Wang, R. (2021). A model-based optimization and control method of slide drilling operations. *Journal of Petroleum Science and Engineering, 198*, 108203. [CrossRef]

[6] Epelle, E. I., & Gerogiorgis, D. I. (2020). A review of technological advances and open challenges for oil and gas drilling systems engineering. *AIChE Journal, 66*(4), e16842. [CrossRef]

[7] Foroud, T., Baradaran, A., & Seifi, A. (2018). A comparative evaluation of global search algorithms in black box optimization of oil production: A case study on Brugge field. *Journal of Petroleum Science and Engineering, 167*, 131-151. [CrossRef]

[8] Zou, C., Zhao, Q., Dong, D., Yang, Z., Qiu, Z., Liang, F., ... & Hu, Z. (2017). Geological characteristics, main challenges and future prospect of shale gas. *Journal of Natural Gas Geoscience, 2*(5-6), 273-288. [CrossRef]

[9] Bai, J., Wang, S., Xu, Q., Luo, Z., Zhang, Z., Lai, K., & Wu, J. (2023). Intelligent real-time predicting method for rock characterization based on multi-source information integration while drilling. *Bulletin of Engineering Geology and the Environment, 82*(4), 150. [CrossRef]

[10] Zhang, K., Wang, C., Tan, F., & Sun, M. (2025). The research progress on shale oil geological analysis driven by big data: Multisource integration methods, key applications, and technical challenges. *Advances in Resources Research, 5*(4), 2702-2742. [CrossRef]

[11] Zhong, R., Johnson, R. L., & Chen, Z. (2019, November). Using machine learning methods to identify coals from drilling and logging-while-drilling LWD data. In *SPE/AAPG/SEG Asia Pacific Unconventional Resources Technology Conference* (p. D012S021R002). URTEC. [CrossRef]

[12] Zang, C., Lu, Z., Ye, S., Xu, X., Xi, C., Song, X., ... & Pan, T. (2022). Drilling parameters optimization for horizontal wells based on a multiobjective genetic algorithm to improve the rate of penetration and reduce drill string drag. *Applied Sciences, 12*(22), 11704. [CrossRef]

[13] Feng, Q., Li, R., Jia, Y., & Liang, Z. (2025). Big data and artificial intelligence-based optimization of petroleum exploration and reservoir modeling: Intelligent pathways for enhancing efficiency and accuracy. *Advances in Resources Research, 5*(2), 477-495. [CrossRef]

[14] Ding, M. (2024, July). Geological characteristics and main controlling factors of the tight sandstone in the Lianggaoshan formation of the Jurassic in the Sichuan Basin. In *Fifth International Conference on Geology, Mapping, and Remote Sensing (ICGMRS 2024)* (Vol. 13223, pp. 35-39). SPIE. [CrossRef]

[15] Li, W., Yue, H., Sun, Y., Guo, Y., Wu, T., Zhang, N., & Chen, Y. (2021). Development evaluation and optimization of deep shale gas reservoir with horizontal wells based on production data. *Geofluids, 2021*(1), 4815559. [CrossRef]

[16] Yang, S., Deng, S., Zhang, Y., Yan, X., Hao, H., Wang, C., & Wang, L. (2023). Research on nano inhibition and plugging potassium amine polysulfonate drilling fluid system to prevent Wellbore instability in deep complex formations. *Petroleum Chemistry, 63*(3), 336-354. [CrossRef]

[17] Li, Y. F., Xu, X. F., Wu, X. H., Zhou, Y., & Pan, J. Y. (2023, September). Development and Application of Friction and Torque Reduction Tools for Extended Reach Well. In *International Field Exploration and Development Conference* (pp. 771-779). Singapore: Springer Nature Singapore. [CrossRef]

[18] Wang, Q., Zhang, L., & Hu, J. (2018). Real-time risk assessment of casing-failure incidents in a whole fracturing process. *Process Safety and Environmental Protection, 120*, 206-214. [CrossRef]

[19] Xiang, J., Wang, X., Lou, W., Wang, X., Zhao, C., & Zhang, F. (2024). Quantitative analysis and modeling of transient cuttings transport impact on drill string mechanics in extended reach drilling. *Processes, 13*(1),

35. [CrossRef]

[20] Hosseini, S., Ghanbarzadeh, A., & Hashemi, A. (2014). Optimization of dogleg severity in directional drilling oil wells using particle swarm algorithm. *Journal of Chemical and Petroleum Engineering*, *48*(2), 139-151. [CrossRef]

[21] Zhou, S. S., Song, J. J., Xu, P., He, M., Xu, M. B., & You, F. C. (2023). A review on tribology, characterization and lubricants for water-based drilling fluids. *Geoenergy Science and Engineering*, *229*, 212074. [CrossRef]

[22] Kanan, M., Al-Nabulsi, D., Alsayed, M., Saleh, Y., Assaf, R., Scelba, G., & Khamis, N. I. (2024). An analytic hierarchy process multi-criteria decision-making model to evaluate renewable energy sources in Palestinian territories. *Operational Research in Engineering Sciences: Theory and Applications*, *7*(1).

[23] Zhang, Y., Wang, Y., Ding, H., Li, Y., & Bai, Y. (2019). Deep well construction of big data platform based on multi-source heterogeneous data fusion. *International Journal of Internet Manufacturing and Services*, *6*(4), 371-388. [CrossRef]

[24] Zhang, H., Yang, S., Liu, D., Li, Y., Luo, W., & Li, J. (2020). Wellbore cleaning technologies for shale-gas horizontal wells: Difficulties and countermeasures. *Natural Gas Industry B*, *7*(2), 190-195. [CrossRef]

[25] Yu, X., Wang, H., Liang, T., Huang, Q., Fan, X., Zhang, Y., ... & Cheremisin, A. (2024, June). Study on the Mechanism of Wellbore Instability in Complex Shale Formations Considering Fault Influence: A Case Study of Fushan Oilfield. In *ARMA US Rock Mechanics/Geomechanics Symposium* (p. D022S024R012). ARMA. [CrossRef]

Yunfeng Hu Received the B.S. degree in petroleum engineering from Southwest Petroleum University, Chengdu, Sichuan, China, in 2005. (Email: 670571747@qq.com)

Ye Yang Received the Ph.D. degree in Energy Science and Engineering from the School of Energy Science and Engineering, Central South University, Changsha 410083, China, in 2024. (Email: Kalimoto1977@yeah.net)